

Water line lists close to experimental accuracy using a spectroscopically determined potential energy surface for H₂¹⁶O, H₂¹⁷O, and H₂¹⁸O

Sergei V. Shirin,¹ Nikolay F. Zobov,¹ Roman I. Ovsyannikov,¹ Oleg L. Polyansky,² and Jonathan Tennyson^{2,a)}

¹*Institute of Applied Physics, Russian Academy of Sciences, Uljanov Street 46, Nizhny Novgorod 603950, Russia*

²*Department of Physics and Astronomy, University College London, Gower Street, London WC1E 6BT, United Kingdom*

(Received 10 March 2008; accepted 22 April 2008; published online 11 June 2008)

Line lists of vibration-rotation transitions for the H₂¹⁶O, H₂¹⁷O, and H₂¹⁸O isotopologues of the water molecule are calculated, which cover the frequency region of 0–20 000 cm⁻¹ and with rotational states up to $J=20$ ($J=30$ for H₂¹⁶O). These variational calculations are based on a new semitheoretical potential energy surface obtained by morphing a high accuracy *ab initio* potential using experimental energy levels. This potential reproduces the energy levels with $J=0, 2$, and 5 used in the fit with a standard deviation of 0.025 cm⁻¹. Linestrengths are obtained using an *ab initio* dipole moment surface. That these line lists make an excellent starting point for spectroscopic modeling and analysis of rotation-vibration spectra is demonstrated by comparison with recent measurements of Lisak and Hodges [J. Mol. Spectrosc. (unpublished)]: assignments are given for the seven unassigned transitions and the intensity of the strong lines are reproduced to within 3%. It is suggested that the present procedure may be a better route to reliable line intensities than laboratory measurements. © 2008 American Institute of Physics. [DOI: 10.1063/1.2927903]

I. INTRODUCTION

Despite half a century of study, work on the spectrum of water vapor shows no sign of diminishing. Recent developments in laboratory spectroscopy¹ and its astrophysical applications² demonstrate the enduring importance and interest in this topic. For the past decade, the major tool for assigning of water spectra was variational calculations based on the use of accurate potential energy surfaces (PESs).^{3,4} As the best *ab initio* determination of the PES (Refs. 5 and 6) still only reproduces the spectrum of water within 1 cm⁻¹, most of this work has been performed using PESs which have first been tuned to reproduce known experimental data.

For a few triatomics, notably H₃⁺,⁷ ozone,⁸ and H₂S,⁹ it has proved possible to develop variational procedures and associated PES, which predict their rotation-vibration transition frequencies with an accuracy close to experimental. Water is particularly challenging both because of the large amplitude of its motion and its relatively low barrier to linearity,¹⁰ features shared in part by the other systems mentioned above, and also because of its uniquely extended vibration-rotation spectrum which is observable even at near ultraviolet wavelengths.¹¹ Indeed, recent experiments¹ have determined vibration-rotation energy levels of water up to 34 000 cm⁻¹ above the ground state and have the capability of extending this range to dissociation.¹² This multiphoton work will not be pursued here.

Literally, hundreds of papers have been published devoted to the experimental observation of water rotation-vibration spectra. These papers generally present data on ex-

perimental line centers and intensities together with the assignment of vibrational and rotational quantum numbers to the observed transitions. For some spectra, such as room temperature pure rotational spectra, the assignment of such quantum numbers is straightforward and does not require variational calculations.¹³ However, for many water spectra, both at room and elevated temperatures, the use of variational calculations provided a major breakthrough in assigning these spectra.^{3,14} This has proved a major stimulus to the development of spectroscopically determined PESs for water of increasing range and accuracy.^{4,15–21}

Even with variational line lists, assignment of water spectra remains far from straightforward with, to take an extreme example, over 80% of the sunspot absorption lines^{22,23} remaining unassigned, despite significant combined laboratory and theoretical work on this problem.^{3,24–26} To make progress on this spectrum, and indeed simpler ones, requires reliable line lists. However, the residual errors in the available calculations means that additional procedures are required to make assignments. A variety of such procedures are in current use including following errors along branches containing a particular class of transitions²⁴ and iterative use of fitted PESs.¹⁶ Some of these methods were codified into expert systems.²⁷ The aim of the present work is to construct a PES, and hence line lists, accurate enough to avoid much of this work and, hence, to significantly simplify and improve the assignment process. To achieve this goal, it is necessary to achieve accuracy close to experimental for the calculated energy levels of the ground electronic state. A loose definition of experimental accuracy could be taken as 0.02 cm⁻¹ since this is the value which approximately characterizes the limit of combination difference discrepancies

^{a)}Electronic mail: j.tennyson@ucl.ac.uk.

for the same levels. Implicitly, such a definition considers that accuracies closer to 0.002 cm^{-1} , usually given by experimentalists as their accuracy, are a bit too optimistic. Such a high accuracy is certainly achievable for strong unblended lines, but most of the lines which are hard to assign do not fall in this category.

So far, the most accurate spectroscopically determined PES for water reproduced the rotation-vibration energy levels of H_2^{16}O , H_2^{17}O , and H_2^{18}O up to $26\,000\text{ cm}^{-1}$ with a standard deviation of 0.07 cm^{-1} .²¹ However, by limiting ourselves to energy levels up to $18\,000\text{ cm}^{-1}$, the goal of achieving experimental accuracy becomes realistic. There are several reasons for this limit. First, use of a lower limit does not improve the fit; indeed, it becomes more and more unstable, as the lack of data makes correlation of the fitted constants a severe limitation on the fitting procedure. Second, $18\,000\text{ cm}^{-1}$ is a natural threshold as it is sufficient to cover the stronger transitions of the 5ν polyad; observations of H_2^{17}O and H_2^{18}O do not extend to higher polyads. Third, the available *ab initio* surfaces become less reliable above $18\,000\text{ cm}^{-1}$, leading to poorer fits.¹ In this work, we therefore present a PES which reproduces the energies of the three isotopologues of water below to $18\,000\text{ cm}^{-1}$ with a standard deviation of 0.02 cm^{-1} ; we also present calculated line lists using this PES for H_2^{16}O , H_2^{17}O , and H_2^{18}O . These are the first line lists of these molecules, which reproduce the spectra with the experimental accuracy. The intensities of the lines were calculated using the new *ab initio* CVR dipole moment surface (DMS).²⁸

The use of an *ab initio* DMS is an important part of this work. Although it is possible to adjust a DMS to experimental data,²⁹ the accuracy with which line intensities can be measured means that this procedure is not really reliable. Indeed, a systematic study of available DMS (Ref. 30) concluded that the use of *ab initio* surfaces gave the most reliable result. To help quantify the accuracy of our calculated intensities, detailed comparisons are made with the recent low-uncertainty laboratory study of Lisak and Hodges.³¹

II. FITTING PROCEDURE

Partridge and Schwenke⁴ were the first to employ a fitting procedure based on the use of an accurate *ab initio* PES as a starting point; this procedure has been used for all subsequent spectroscopically determined PESs of water. Here, we start from the very accurate *ab initio* calculations used to construct the CVRQD PES.^{5,6} To construct this surface, multireference configuration interaction (MRCI) calculations using an aug-cc-pCV6Z basis set were performed at 1495 geometries. These points were extrapolated to the complete basis set (CBS) limit and several corrections added: a corevalence correction due to Partridge and Schwenke⁴ as well as the adiabatic, relativistic, and quantum electrodynamics corrections.^{5,6} These corrections are all used here, which implies a slightly different PES for each isotopologue. We employ 1107 of the CBS MRCI points to produce the *ab initio* PES, which was used as a starting potential for fitting procedure. We call the resulting *ab initio* surface as PES367. This surface reproduces the selected *ab initio* points with a stan-

dard deviation of 0.56 cm^{-1} . For its construction, we use the same analytical form used for the CVRQD PES (Ref. 6) and 240 parameters. PES367 was obtained after we tested many different selections of points; the 1107 points, which we finally chose, provided the starting point for a fitted potential that reproduced levels up to $26\,000\text{ cm}^{-1}$ with a standard deviation of 0.03 cm^{-1} .¹ PES367 not only was used as a starting point in Ref. 1 but also produced a D_2O line list accurate to about 0.02 cm^{-1} as well.²⁰ A FORTRAN version of PES367 is given, along with the spectroscopically determined PESs derived below, in EPAPS.³²

All nuclear motion calculations were performed using the program suite DVR3D,³³ in Radau coordinates. These calculations all used 29 radial grid points and 40 angular grid points. Vibrational Hamiltonian matrices with final dimension of 1500 were diagonalized; for the rotational problems, the final matrices had dimension of $400(J+1-p)$, where J is the total angular momentum quantum number and p is the parity. This is sufficient to give well converged results for all energies of interest. Nuclear masses were used for all calculations.

The observed energy levels for H_2^{17}O and H_2^{18}O were obtained using the MARVEL procedure,³⁴ which inverts the information contained in assigned experimental rotation-vibration transitions to obtain measured energy levels. This work was performed as part of a comprehensive study of the energy levels of water isotopologues, and full results will be reported elsewhere.³⁵ The combined number of measured and assigned transitions for the H_2^{17}O and H_2^{18}O molecules is less than 30 000. This number for H_2^{16}O molecule is at least an order of magnitude bigger. The task of gathering all H_2^{16}O transitions and then obtaining the measured levels is quite formidable and will take some time; indeed, it is intended that the results presented here will be used as part of this work both to check the results and to aid further assignments. For the present fit, we therefore used energies from the previous H_2^{16}O compilation³⁶ as adjusted by our previous study,²¹ where considerable efforts were made to construct a reliable data set of energy levels without possible misassignments.

The final set of experimental energies used for the fit consists of 2287 levels with $J=0, 2$, and 5 up to $18\,000\text{ cm}^{-1}$ for the three isotopologues. This set contains about 900 more energy levels below $18\,000\text{ cm}^{-1}$ than there were used in our previous study²¹ due to new experimental studies;³⁷ the experimental data used are summarized in Ref. 34.

For the fitting procedure, we have used the same general functional form as in our previous works,^{16,17,20,21} that of a morphing function, which we fit, times an *ab initio* PES, as

$$V_{\text{fit}}(r_1, r_2, \theta) = f_{\text{morp}}(r_1, r_2, \theta) V_{\text{ab initio}}(r_1, r_2, \theta). \quad (1)$$

For our fits, the morphing function was expressed as a power series in the so-called Jensen coordinates,

$$s_1 = \frac{r_1 + r_2}{2} - r_e,$$

$$s_2 = \cos \theta - \cos \theta_e,$$

TABLE I. Fit coefficients, $c_{i,j,k}$, of the morphing function [Eq. (1)]. Dimensions are $a_0^{-(i+k)}$.

$i j k$	$c_{i,j,k}$
0 0 0	1.000 078 882 355 936
1 1 0	-0.002 415 812 266 162
2 0 0	0.002 240 376 726 999
3 0 0	0.002 002 058 839 135
0 0 2	0.004 352 410 367 155
4 0 0	-0.015 704 117 909 675
0 2 0	-0.000 836 461 582 832
0 3 0	-0.000 223 101 870 130
0 4 0	-0.000 006 450 294 159
2 1 0	0.008 835 194 672 647
1 2 0	-0.001 332 128 652 146
1 0 2	0.001 280 889 063 142
0 1 2	0.002 101 151 639 495
0 0 4	-0.014 154 869 803 467
3 1 0	-0.020 036 943 727 003
1 3 0	0.003 848 424 509 110
2 2 0	0.003 459 398 217 948
2 0 2	-0.000 025 023 375 137
1 1 2	0.008 773 551 596 677
0 2 2	-0.004 784 657 116 544
5 0 0	0.0174 704 264 114 97
0 5 0	-0.000 051 405 936 565
4 1 0	0.004 179 689 849 942
3 0 2	-0.002 405 948 907 299

$$s_3 = \frac{r_1 - r_2}{2}, \quad (2)$$

$$f_{\text{morph}} = c_{000} + \sum_{ijk} c_{ijk} s_1^i s_2^j |s_3^k|, \quad 2 \leq i + j + k \leq N. \quad (3)$$

We performed a series of calculations with different morphing functions to help choose the optimal set of parameters. In particular, we tested all fourth-order ($N=4$) terms as well as the effect of including fifth-order ($N=5$) terms. We have tried to minimize the number of these parameters as extra parameters could lead to wrinkles in the surface and worsen the interpolation qualities of it. This means that the high accuracy of the fitted PES is due to the high quality *ab initio* surface but not because of the large number of fitted parameters. This strategy differs from that used in some other high accuracy fits.⁹ The final set of terms is given in Table I.

We note that the use of a polynomial for the morphing function may cause the potential to show unphysical behavior for large (or indeed very small) internuclear separations. The whole issue of how to define an accurate global potential for water is a difficult one, which we recently started to address.³⁸ For present purposes, it is sufficient to say that our new fitted potential is designed to characterize the region up to 18 000 cm^{-1} and should not be assumed to be reliable at energies significantly above this value.

Optimization of 24 parameters in the morphing function allowed us to reproduce the experimental data with a standard deviation of 0.025 cm^{-1} . The constants of the morphing

function used to determine the fitted potential are given in Table I. Due to symmetry considerations, only even powers of k were included in the fit.

To allow for nonadiabatic effect on highly excited rotational levels, we, as before,²¹ used the additional J_{xx} , J_{yy} , and J_{zz} operators defined by Schwenke.³⁹ These operators were scaled based on an analysis of the errors in the predicted energy levels with $J=20$ and $J=40$ for the PES obtained by fitting only levels with $J=0, 2$, and 5. This analysis gave scaling factors of 0.30 for J_{xx} , 0.5 for J_{yy} , and -0.24 for J_{zz} . As noted previously,²¹ the value of this scaling is very sensitive to the precise PES it is employed with. Use of these rotationally nonadiabatic terms leads to a standard deviation of 0.1 cm^{-1} for levels with $J=20$ and 0.3 cm^{-1} for those with $J=40$.

III. LABELING

It is a standard practice to use quantum numbers that serve to identify the energy levels and lines in a spectrum. To aid the use of our line lists, each transition has a full quantum number assignment. However, achieving this is not altogether straightforward.

Every state of any of the three molecules H_2^{16}O , H_2^{17}O , and H_2^{18}O can be described by a rigorous set of quantum numbers responsible for the symmetry of the wave function: these are J , p and whether the state is ortho or para. The addition of the level number within a symmetry block is enough to completely characterize each state. These quantum numbers are automatically assigned to energy levels by the DVR3D programs.³³ However, the conventional quantum numbers for water are J , K_a , K_c , v_1 , v_2 , and v_3 . These labels, which are based on the rigid rotor-harmonic oscillator model, are more informative from the viewpoint of the physics of transitions from one level to another. The quantum numbers K_a , K_c , v_1 , v_2 , and v_3 are approximate, and the assignment of these labels to energy levels by different methods may be ambiguous in some cases and depend on the method used. The assignment of approximate labels is a separate problem not addressed by the DVR3D program suite.

Since the structures of the energy levels of water with different oxygen isotopes are similar, we first label the levels of the H_2^{16}O molecule. The primary method used is based on the analysis of the dependence of the energy levels on the labels⁴⁰ and is performed in two stages. The first stage is to label the vibrational ($J=0$) energy levels; for this, we used the quasiharmonicity of the molecule. For a harmonic oscillator with three degrees of freedom, the energy can be expressed as

$$E = v_1\omega_1 + v_2\omega_2 + v_3\omega_3, \quad (4)$$

where v_1 , v_2 , and v_3 are the vibrational quantum numbers and ω_1 , ω_2 , and ω_3 are the fundamental frequencies. The energy here is measured from the energy of the ground state. However, the real molecule is not a harmonic oscillator. Therefore, our labeling method dealt with the effective fundamental frequencies,

$$\omega_1^{\text{eff}} = E(v_1, v_2, v_3) - E(v_1 - 1, v_2, v_3),$$

$$\omega_2^{\text{eff}} = E(v_1, v_2, v_3) - E(v_1, v_2 - 1, v_3),$$

$$\omega_3^{\text{eff}} = E(v_1, v_2, v_3) - E(v_1, v_2, v_3 - 1). \quad (5)$$

The effective frequencies themselves are functions of v_1 , v_2 , and v_3 . These functions vary smoothly, and they are the key functions for the prediction of the energy levels from the previous already labeled levels. Each energy level $E(v_1, v_2, v_3)$ can be predicted on the basis of three (or less if some $v_i=0$) previous levels: $E(v_1-1, v_2, v_3)$, $E(v_1, v_2-1, v_3)$, and $E(v_1, v_2, v_3-1)$, taking into account the current values of the effective frequencies. To increase the accuracy of the assignment in some cases, experimental values were used as predictions. For each predicted level, one of the closest calculated energy levels of the correct symmetry was selected. The labels v_1 , v_2 , v_3 were assigned to this calculated level, and then new effective frequencies were calculated. The second stage involves labeling the vibrational-rotational energy levels with $J>0$. The total energy of a level can roughly be represented as a sum of the vibrational and rotational energies. For the second stage, we used the empirical observation that the rotational energy depends weakly on the vibrational quantum numbers; for a given set of constant rotational quantum number and a smooth change of vibrational quantum numbers, the rotational part of the energy changes smoothly.

To eliminate ambiguities in the selection of the calculated level corresponding to the given set of labels, the following considerations were used. For a particular energy level, the properly assigned set of labels is that corresponding to the set obtained from the analysis of the experimental energy level (if available) or, otherwise, for which the absolute value of the difference between the predicted and calculated values is the smallest. The accurate labeling of the vibrational levels (first $J=0$ stage) is more important than at the second stage since, as the second stage also depends on this, any error in the assignment of the vibrational labels spawns errors in the labels of levels with $J>0$. Therefore, each vibrational level below $20\,000\text{ cm}^{-1}$ was labeled manually. Other methods were used to eliminate any ambiguities and to check the ultimate label. One method used for checking is based on the analysis of wave functions.⁴¹

The (small amplitude) vibrations of a molecule near equilibrium can be divided into independent vibrations along each normal coordinate. The Hamiltonian of a multidimensional harmonic oscillator in normal coordinates is a sum of one-dimensional Hamiltonians, and the multidimensional wave function is a product of one-dimensional wave functions. For normal coordinates, the diagonal element of the matrix of any square coordinate can be expressed through the degree of excitation along only this coordinate,

$$\langle X_v^2 \rangle = \left(v + \frac{1}{2}\right) (\hbar/\mu\omega). \quad (6)$$

The diagonal matrix elements were calculated by the numerical integration of the corresponding wave functions. Since the wave functions in the vibrational states (000), (100), (010), and (001) can be easily identified, we determined from these states the normalization coefficients ($\hbar/\mu\omega_i$) for each normal coordinate. We then calculated the vibrational quan-

tum numbers, which are rounded to the nearest integer, using the matrix elements $\langle X_v^2 \rangle$. Jensen coordinates [Eq. (2)], which are close to the normal ones, were used. This method is not as accurate as the basic one but provides an important check. Assignment of vibrational labels to levels with large values of v_2 , corresponding to the bending vibrations, is the most doubtful. We therefore used one further method to analyze the value of this quantum number by adding a term to the potential that depends only on the angle.⁴² The artificial addition of this term to the PES shifts the calculated energy levels, and the larger the value of v_2 , the larger this shift. Comparison of calculations with and without the additional term allows us to estimate v_2 . This method is also not completely reliable, but the combination of the different methods provides a more accurate set of labels than can be obtained from only one method.

The labeling of energy levels of H_2^{17}O and H_2^{18}O by the method similar to that used for H_2^{16}O appears to be less efficient. For these molecules, there are significantly less experimental data, which are needed for the refinement of the effective frequencies. Without this refinement, inaccuracies in the prediction process accumulate, which can significantly increase the number of mislabeled levels. In the structure of their energy levels, the H_2^{17}O and H_2^{18}O molecules are more similar to H_2^{16}O than D_2^{16}O .²⁰ Since the oxygen nucleus lies near the molecular center of mass, the relatively small changes of its mass only lead to small changes in the principal moments of inertia and, consequently, the rotational energies. The addition of neutrons to the oxygen nucleus affects the structure of the energy levels much more weakly than the addition of neutrons to the hydrogen nucleus. Therefore, for the H_2^{17}O and H_2^{18}O isotopologues, the labels were assigned on the basis of those labels already assigned to the energy levels of H_2^{16}O . Since each set of energy levels is divided into blocks on the basis of their rigorous quantum numbers, and levels in each block are energy ordered, it is easy to make the correspondence between the levels of H_2^{16}O and two other isotopologues H_2^{17}O and H_2^{18}O . In most cases, this correspondence means the coinciding labels. Unfortunately, labeling by direct correspondence is incorrect in some cases. Such errors were corrected by the above described methods and also using the fact that the difference in the energies of the levels $E(\text{H}_2^{18}\text{O}) - E(\text{H}_2^{17}\text{O})$ is almost equal to $E(\text{H}_2^{17}\text{O}) - E(\text{H}_2^{16}\text{O})$ for each set of quantum numbers.

It should be noted here that our labeling procedure, as with all methods of “determining” approximate quantum numbers, is not free from error. When the line list is used during the assignment of experimental spectra, other factors should also be taken into account, for example, the dependence of the transition intensities on the quantum numbers. Finally, we should note that a very few, less than 0.01%, of the levels remained unlabeled at the end of this process. These levels are characterized by negative quantum numbers in our final line lists.

IV. LINE LIST CALCULATION

Table II presents our calculated vibrational band origins for the three isotopologues considered and compares them

TABLE II. Calculated band origins of H₂¹⁶O, H₂¹⁷O, and H₂¹⁸O and differences between observed, if available, and calculated values in cm⁻¹. Observed values are from Refs. 34–36.

$v_1 v_2 v_3$	H ₂ ¹⁶ O		H ₂ ¹⁷ O		H ₂ ¹⁸ O	
	E_{calc}	Obs.–Calc.	E_{calc}	Obs.–Calc.	E_{calc}	Obs.–Calc.
0 1 0	1 594.758	–0.012	1 591.327	–0.001	1 588.268	0.008
0 2 0	3 151.645	–0.015	3 144.987	–0.007	3 139.049	0.001
1 0 0	3 657.068	–0.015	3 653.159	–0.017	3 649.704	–0.019
0 0 1	3 755.892	0.037	3 748.277	0.041	3 741.522	0.045
0 3 0	4 666.805	–0.014	4 657.123		4 648.488	–0.028
1 1 0	5 234.943	0.032	5 227.665	0.040	5 221.208	0.032
0 1 1	5 331.259	0.008	5 320.228	0.023	5 310.426	0.034
0 4 0	6 134.018	–0.003	6 121.552		6 110.433	
1 2 0	6 775.068	0.025	6 764.693	0.033	6 755.472	0.038
0 2 1	6 871.518	0.002	6 857.257	0.016	6 844.573	0.025
2 0 0	7 201.561	–0.021	7 193.268	–0.021	7 185.903	–0.033
1 0 1	7 249.814	0.005	7 238.707	0.007	7 228.870	0.010
0 0 2	7 445.040	0.005	7 431.070	0.006	7 418.708	0.012
0 5 0	7 542.385	0.085	7 527.495		7 514.208	
1 3 0	8 274.000	–0.023	8 260.796		8 249.050	
0 3 1	8 373.855	–0.003	8 356.525		8 341.099	
2 1 0	8 761.529	0.050	8 749.850		8 739.465	
1 1 1	8 806.981	0.019	8 792.515	0.029	8 779.681	0.039
0 6 0	8 870.165		8 853.496		8 838.615	
0 1 2	9 000.150	–0.010	8 982.865	0.004	8 967.546	
1 4 0	9 724.252		9 708.580		9 694.629	
0 4 1	9 833.571	0.016	9 813.335		9 795.316	0.014
0 7 0	10 086.179		10 068.204		10 052.171	
2 2 0	10 284.322	0.047	10 269.615		10 256.526	0.059
1 2 1	10 328.718	0.012	10 311.180	0.023	10 295.603	0.031
0 2 2	10 521.762		10 501.347		10 483.232	–0.011
3 0 0	10 599.691	–0.004	10 586.057		10 573.928	–0.011
2 0 1	10 613.345	0.008	10 598.463	0.013	10 585.275	0.010
1 0 2	10 868.900	–0.024	10 853.528	–0.023	10 839.976	–0.020
0 0 3	11 032.419	–0.015	11 011.888		10 993.683	–0.002
1 5 0	11 098.417		11 080.531		11 064.604	
0 5 1	11 242.727		11 219.801		11 199.380	
0 8 0	11 253.686		11 232.314		11 213.304	
2 3 0	11 767.374	0.014	11 749.990		11 734.507	0.018
1 3 1	11 813.222	–0.017	11 792.831	–0.005	11 774.707	
0 3 2	12 007.790	–0.014	11 984.350		11 963.534	0.004
3 1 0	12 139.273	0.043	12 122.162		12 106.936	0.042
2 1 1	12 151.214	0.039	12 132.947		12 116.743	0.072
1 6 0	12 380.481		12 357.871		12 337.595	
1 1 2	12 407.635	0.026	12 389.063		12 372.663	0.042
0 9 0	12 533.638		12 509.428		12 488.021	
0 1 3	12 565.033	–0.027	12 541.239		12 520.120	0.003
0 6 1	12 586.189		12 560.947		12 538.458	
2 4 0	13 204.805		13 185.199		13 167.723	
1 4 1	13 256.170		13 233.165		13 212.703	
0 4 2	13 453.507		13 427.151		13 403.732	
3 2 0	13 640.639		13 620.562		13 602.656	
2 2 1	13 652.619	0.039	13 631.458	0.042	13 612.662	0.048
1 7 0	13 660.305		13 637.808		13 617.644	
4 0 0	13 828.278		13 808.239		13 784.213	
3 0 1	13 830.942	–0.005	13 809.739		13 793.274	–0.016
0 7 1	13 835.335	0.038	13 812.168		13 795.414	
0 10 0	13 857.238		13 826.116		13 798.557	
1 2 2	13 910.879	0.002	13 889.427		13 870.456	
0 2 3	14 066.191	0.005	14 039.335		14 015.479	
2 0 2	14 221.132	0.027	14 203.538		14 187.975	0.007
1 0 3	14 318.823	–0.010	14 296.287	–0.007	14 276.341	–0.005
0 0 4	14 537.448	0.056	14 511.346		14 488.215	

TABLE II. (Continued.)

$v_1 v_2 v_3$	$\text{H}_2 \text{ }^{16}\text{O}$		$\text{H}_2 \text{ }^{17}\text{O}$		$\text{H}_2 \text{ }^{18}\text{O}$	
	E_{calc}	Obs. – Calc.	E_{calc}	Obs. – Calc.	E_{calc}	Obs. – Calc.
2 5 0	14 578.683		14 557.642		14 538.890	
1 5 1	14 647.942	0.035	14 622.660		14 600.161	
1 8 0	14 818.852		14 792.382		14 768.669	
0 5 2	14 881.591		14 854.740		14 831.051	
0 8 1	14 983.787		14 954.457		14 928.349	
3 3 0	15 108.075		15 085.368		15 065.130	
2 3 1	15 119.004	0.027	15 095.134		15 073.918	
0 11 0	15 294.832		15 257.235		15 223.730	
4 1 0	15 344.497	0.007	15 322.523		15 303.015	
3 1 1	15 347.948	0.010	15 325.604		15 305.789	
1 3 2	15 377.725		15 353.549		15 332.147	
0 3 3	15 534.673	0.034	15 504.861		15 478.360	
2 1 2	15 742.765	0.038	15 721.916		15 703.450	
1 1 3	15 832.764	0.016	15 807.050		15 784.269	
2 6 0	15 869.782		15 846.110		15 825.032	
1 6 1	15 968.883		15 941.227		15 916.597	
0 1 4	16 046.895		16 017.675		15 991.761	
1 9 0	16 072.422		16 042.903		16 016.658	
0 9 1	16 160.184		16 126.445		16 096.439	
0 6 2	16 215.093		16 183.667		16 155.740	
3 4 0	16 534.256		16 509.329		16 487.090	
2 4 1	16 546.279	0.040	16 520.028		16 496.676	
1 4 2	16 795.754		16 769.578		16 742.514	
3 2 1	16 821.638	-0.004	16 781.991	0.008	16 748.612	
4 2 0	16 823.072		16 797.160		16 775.378	
0 12 0	16 824.295		16 798.863		16 776.787	
5 0 0	16 898.393		16 875.244		16 854.772	
4 0 1	16 898.816	0.025	16 875.598	0.023	16 855.070	
0 4 3	16 967.393		16 934.702		16 905.629	
2 7 0	17 137.860		17 112.037		17 088.999	
2 2 2	17 227.336	0.044	17 199.886		17 173.298	
1 7 1	17 229.695		17 203.680		17 182.702	
1 2 3	17 312.553	-0.002	17 284.082		17 258.827	
1 10 0	17 383.225		17 348.052		17 316.840	
0 10 1	17 444.480		17 405.942		17 371.680	
3 0 2	17 458.246	-0.032	17 436.290		17 416.760	
0 7 2	17 491.035		17 457.283		17 427.286	
2 0 3	17 495.476	0.052	17 470.476		17 448.348	
0 2 4	17 526.306		17 494.212		17 465.730	
1 0 4	17 747.975		17 721.602		17 698.341	
3 5 0	17 911.165		17 884.765		17 861.175	
2 5 1	17 927.890		17 899.633		17 874.477	
0 0 5	17 948.411		17 916.830		17 888.819	
1 5 2	18 161.426		18 133.200		18 108.177	
3 3 1	18 265.815		18 238.782		18 214.723	

with experimental data, where available. It is apparent that our PES reproduces the observed data closely over the whole energy range considered. Our predictions for the many vibrational levels that have yet to be observed are likely to be very reliable, particularly for cases where the corresponding level has already been observed for another isotopologue.

To facilitate the analysis of new experimental spectra of water vapor, we have calculated transitions line lists for the $\text{H}_2 \text{ }^{17}\text{O}$ and $\text{H}_2 \text{ }^{18}\text{O}$ isotopologues in the 0–20 000 cm^{-1} range with J values up to 20 and up to $J=30$ for $\text{H}_2 \text{ }^{16}\text{O}$ with a temperature of 296 K. There are a number of high tempera-

ture (3000 K) spectra of water vapor, in particular, sun spot spectra and torch spectra. So, we have also calculated the line lists up to the same J values for the three isotopologues with the temperature of 3000 K, for which we used the partition function from Vidler and Tennyson.⁴³ For the intensity calculations, we used the CVR DMS of Lodi *et al.*²⁸ The line list and PES used in the calculations are given in the electronic archive EPAPS.³² An intensity cutoff of 1.0×10^{-30} cm molecule^{-1} was used for temperatures of 296 and 3000 K; the resulting line lists have nearly 220 000 lines each at 296 K and over 18 000 000 lines each for $\text{H}_2 \text{ }^{17}\text{O}$ and

TABLE III. Sample transition from the H₂¹⁶O line list with explanation.

Number	1 ^a	2 ^b	3 ^c	4 ^d	5 ^e	6 ^f	7 ^g	8 ^h	9 ⁱ	10 ^j	11 ^k	12 ^l	13 ^m	14 ⁿ	15 ^o	16 ^p	17 ^q	18 ^r	19 ^s	20 ^t	21 ^u	22 ^v	23 ^w	24 ^x	25 ^y	26 ^z
Value	1	6	0	1	5	0	2	447.2477	446.511	0.735615	0.20	0.440 × 10 ⁻²⁴	0.316 × 10 ⁻⁶	0.197 × 10 ⁻⁸	6	1	6	0	0	0	5	2	3	0	0	0

^aLevel's vibration symmetry: 0, symmetric states; 1, asymmetric states.

^bUpper level quantum number J .

^cUpper level rotation symmetry (0 or 1).

^dUpper level number in current block.

^eLower level quantum number J .

^fLower level rotation symmetry (0 or 1).

^gLower level number in current block.

^hUpper level energy value (cm⁻¹).

ⁱLower level energy value (cm⁻¹).

^jTransition frequency (cm⁻¹).

^kSquared transition dipole moment (D²).

^lAbsolute line intensity, which shows absorption by one molecule (cm molecules⁻¹).

^mRelative transition intensity (normalized by the maximum transition intensity).

ⁿEinstein's coefficient (s⁻¹).

^oUpper level quantum number J .

^pUpper level quantum number K_a .

^qUpper level quantum number K_c .

^rUpper level quantum number v_1 .

^sUpper level quantum number v_2 .

^tUpper level quantum number v_3 .

^uLower level quantum number J .

^vLower level quantum number K_a .

^wLower level quantum number K_c .

^xLower level quantum number v_1 .

^yLower level quantum number v_2 .

^zLower level quantum number v_3 .

H₂¹⁸O at 3000 K. The more extensive hot H₂¹⁶O line list contains 23 425 730 transitions. These line lists should be sufficient for analyzing room temperature and hot experimental spectra. Table III presents a sample of our calculated line list with an explanation of the output format. The line list is available for downloads from the URL address.

The calculated line lists for the three major isotopologues of water are the most accurate line list so far both in terms of line centers and line intensities. Figure 1 illustrates this point by comparing a portion of the visible wavelength spectrum of Fally *et al.*⁴⁴ with results from our line list. This high frequency region was chosen precisely because it was at such frequencies that previous line lists have struggled to give good results for both line positions and intensities. This figure demonstrates visually what an accuracy of about 0.02 cm⁻¹ means. The calculated line centers coincide with the experimental ones within the observed linewidth. This means that a semiautomatic assignment procedure for such spectra, whose assignment recently constituted a major project in its own right,⁴⁵ should now be possible using the

line lists of this paper. In other words, the lack of ambiguity between experimental and calculated lines should mean that no expert evaluation of the assignment is required and full line assignment is straightforward. This should both facilitate significantly the assignment procedure and will contribute to the accuracy of the models of water absorption for terrestrial or stellar atmospheres, which could be built upon our line lists.

To illustrate this point, we have analyzed the recent spectrum of Lisak and Hodges.³¹ This work studied 74 transitions in the 930 nm (10 700 cm⁻¹) region, 7 of which remain unassigned. Table IV gives our assignments for these lines.

The main focus of Lisak and Hodges' study³¹ was on trying to reduce the uncertainty with which experimental line intensities could be measured. Their study should therefore provide a benchmark against which our results can be tested. Table V compares our results with theirs.

Lisak and Hodges divide their study into 23 relatively strong lines, whose intensity was determined to within 1%,

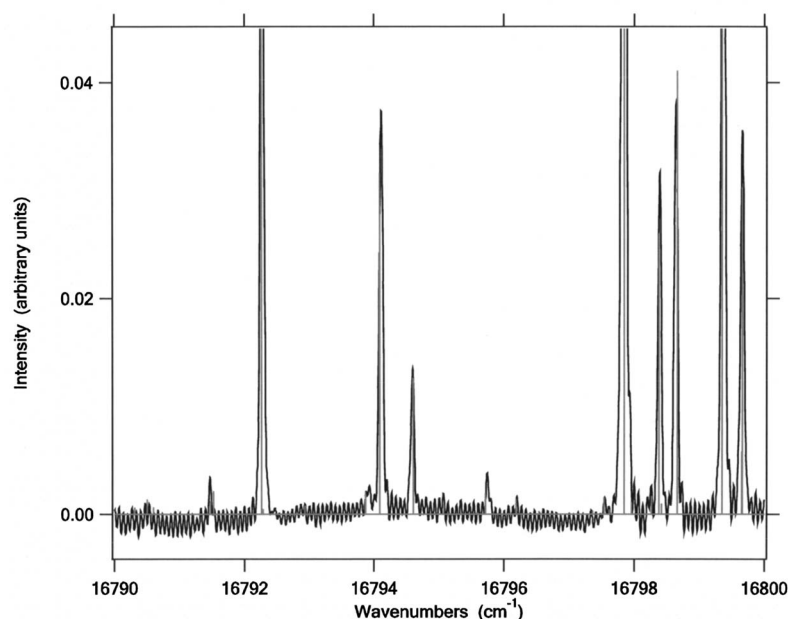


FIG. 1. Visible wavelength absorption spectrum of water recorded by Fally *et al.* (Ref. 44). Vertical lines give the corresponding spectrum predicted by the H₂¹⁶O line list of the present work.

TABLE IV. Assignments for the unassigned lines observed by Lisak and Hodges (Ref. 31).

Obs.		Calc.					
Frequency (cm ⁻¹)	Obs. Intensity (cm ² cm ⁻¹ molecule ⁻¹)	Frequency (cm ⁻¹)	Calc. Intensity (cm ² cm ⁻¹ molecule ⁻¹)	$J' K_a' K_c'$	$v_1' v_2' v_3'$	$J K_a K_c$	$v_1 v_2 v_3$
10 691.981 73	$5.25(64) \times 10^{-26}$	10 691.95	1.10×10^{-26}	9 2 8	211	8 2 7	010
10 692.914 97	$1.87(27) \times 10^{-26}$	10 692.99	1.72×10^{-26}	10 3 8	022	10 2 9	000
10 736.666 75	$1.52(40) \times 10^{-26}$	10 736.72	1.01×10^{-26}	8 7 2	300	9 4 5	000
10 737.044 03	$8.2(2.2) \times 10^{-27}$	10 736.98	8.42×10^{-27}	9 7 2	140	8 6 3	000
10 737.411 86	$4.4(1.8) \times 10^{-27}$	10 737.49	3.92×10^{-27}	9 3 7	300	8 2 6	000 ^a
10 737.598 47	$2.7(3.0) \times 10^{-27}$	10 737.67	2.24×10^{-27}	13 6 7	022	12 7 6	000
10 834.200 62	$1.39(60) \times 10^{-27}$	10 834.22	1.02×10^{-27}	3 3 0	013	4 3 1	010

^aH₂¹⁸O line, intensity for natural abundance.

and a set of weak lines for which their results are systematically stronger than previous studies. If one excludes the two weakest of the “strong” lines, our line list predicts the measured intensities to within about 3%. Indeed, the fact that our lines are systematically about 3% too strong is in line with the previous calculations using the CVR dipole, which made such comparisons at longer wavelengths.²⁸

We do not give comparison for all the 50 or so weaker

transitions since this merely confirms Lisak and Hodges’s comment that their measurements appear to overestimate the intensity of these lines by some 20%. Instead, we give a comparison for two classes of lines that are weak not because of their intrinsic band strength: high- J lines that are weak because of their Boltzmann factor and H₂¹⁸O lines that are weak due to its reduced natural abundance. In both these cases, our line list would be expected to give results of simi-

TABLE V. Comparison of measured (Ref. 31) and calculated intensities in cm² cm⁻¹ molecule⁻¹.

Frequency (cm ⁻¹)	$v_1' v_2' v_3'$	$v_1 v_2 v_3$	$J' K_a' K_c'$	$J K_a K_c$	I_{obs}	I_{calc}	$I_{\text{obs}} - I_{\text{calc}}$ (%)
H ₂ ¹⁶ O strong lines							
10 603.529	201	000	2 2 0	2 2 1	$5.899(34) \times 10^{-22}$	5.73×10^{-22}	2.86
10 605.044	201	000	1 1 1	1 1 0	$4.348(25) \times 10^{-22}$	4.25×10^{-22}	2.25
10 605.180	201	000	3 2 1	3 2 2	$0.8398(79) \times 10^{-22}$	8.36×10^{-23}	0.45
10 656.750	201	000	2 0 2	1 0 1	$5.349(51) \times 10^{-22}$	5.21×10^{-22}	2.59
10 660.711	201	000	2 1 1	1 1 0	$4.309(26) \times 10^{-22}$	4.18×10^{-22}	2.99
10 667.763	201	000	3 1 3	2 1 2	$6.168(38) \times 10^{-22}$	5.97×10^{-22}	3.21
10 670.122	201	000	3 2 2	2 2 1	$3.057(17) \times 10^{-22}$	2.97×10^{-22}	2.84
10 673.529	201	000	3 0 3	2 0 2	$2.190(14) \times 10^{-22}$	2.13×10^{-22}	2.73
10 683.380	201	000	4 1 4	3 1 3	$2.165(14) \times 10^{-22}$	2.10×10^{-22}	3.00
10 683.697	201	000	4 3 1	3 3 0	$1.5015(89) \times 10^{-22}$	1.46×10^{-22}	2.76
10 687.362	201	000	4 0 4	3 0 3	$6.433(40) \times 10^{-22}$	6.26×10^{-22}	2.68
10 697.416	201	000	5 1 5	4 1 4	$5.476(33) \times 10^{-22}$	5.31×10^{-22}	3.03
10 698.944	201	000	4 2 2	3 2 1	$3.631(20) \times 10^{-22}$	3.54×10^{-22}	2.50
10 700.672	201	000	4 1 3	3 1 2	$4.829(31) \times 10^{-22}$	4.68×10^{-22}	3.08
10 700.841	201	000	5 3 3	4 3 2	$1.702(19) \times 10^{-22}$	1.63×10^{-22}	4.23
10 704.420	201	000	5 2 4	4 2 3	$3.223(26) \times 10^{-22}$	3.18×10^{-22}	1.33
10 711.089	201	000	6 0 6	5 0 5	$3.948(29) \times 10^{-22}$	3.87×10^{-22}	1.97
10 730.107	102	000	5 0 5	6 1 6	$0.1440(50) \times 10^{-22}$	1.07×10^{-23}	25.6
10 730.228	201	000	7 2 6	6 2 5	$1.4270(80) \times 10^{-22}$	1.36×10^{-22}	4.69
10 730.424	201	000	6 1 5	5 1 4	$2.121(13) \times 10^{-22}$	2.04×10^{-22}	3.81
10 731.011	201	000	8 0 8	7 0 7	$1.3121(88) \times 10^{-22}$	1.27×10^{-22}	3.20
10 731.166	102	000	2 1 2	3 2 1	$0.0537(33) \times 10^{-22}$	3.75×10^{-24}	30.1
10 731.399	201	000	8 1 8	7 1 7	$0.5017(40) \times 10^{-22}$	4.86×10^{-23}	3.12
H ₂ ¹⁶ O weak lines with high J							
10 692.147	201	000	11 3 9	11 1 10	$1.278(74) \times 10^{-25}$	1.01×10^{-25}	20.9
10 693.201	201	000	12 2 10	12 2 11	$4.6(1.3) \times 10^{-26}$	3.23×10^{-26}	29.8
10 693.562	201	000	12 3 10	12 1 11	$9.9(8.9) \times 10^{-27}$	8.60×10^{-27}	13.1
H ₂ ¹⁸ O weak lines							
10 671.114	201	000	5 0 5	4 0 4	$4.11(21) \times 10^{-25}$	3.44×10^{-25}	16.3
10 671.146	201	000	4 2 2	3 2 1	$8.40(42) \times 10^{-25}$	6.91×10^{-25}	17.7
10 693.066	201	000	7 1 7	6 1 6	$6.81(34) \times 10^{-25}$	4.85×10^{-25}	28.8
10 693.276	201	000	7 0 7	6 0 6	$2.039(72) \times 10^{-25}$	1.66×10^{-25}	18.6

lar accuracy to those obtained for the strong lines since the actual linestrengths are not small and the factors reducing the intensity are multiplicative ones that are introduced *post hoc* when synthesizing the spectrum. It can be seen that for these weak lines, our predicted intensities are some 20% lower than the observed ones. This confirms that higher intensities measured by Lisak and Hodges for these weak lines do indeed appear to be an artifact of their experiment.

V. CONCLUSION

A high accuracy PES for the electronic ground state of water is obtained using a state-of-the-art *ab initio* PES as a starting point and a morphing function fitted, so that the PES reproduced the experimental energy levels. This PES is used to calculate line lists for H_2^{16}O , H_2^{17}O , and H_2^{18}O , which can be used to model the water spectra for frequencies up to $18\,000\text{ cm}^{-1}$. The accuracy of the predicted line positions is determined by the accuracy of PES employed. The accuracy of intensity calculations is largely determined by the CVR DMSs (Ref. 28) used in the calculations and is virtually independent of the accuracy of the PES for the majority of lines. Our analysis combined with that given previously^{28,46} suggests that this *ab initio* DMS is capable in predicting the intensity of the majority of water transitions within about 3%. Given the difficulty of measuring water line intensities to high accuracy, and the clear improvements to the procedure for calculating an *ab initio* DMS already suggested,²⁸ it is by no means fanciful to suggest that improved *ab initio* calculations probably represent the best prospect of obtaining intensities for the bulk of water transitions of importance to an accuracy of 1%.

There are many important applications for an accurate water line list. Models of the absorption processes in both terrestrial and cool stellar atmospheres are examples, although the latter needs a more extended line list than the ones presented here.⁴⁷ However, the most obvious use of the line lists is for the assignment of the experimentally observed spectra of water which remains an active topic of study.^{46,48}

Until now, the most accurate generally available spectroscopically determined PES for water is FIS3,²¹ which reproduces the observed rotation-vibration energy levels of H_2^{16}O , H_2^{17}O , and H_2^{18}O up to $26\,000\text{ cm}^{-1}$ with a standard deviation of 0.07 cm^{-1} .²¹ This standard deviation was actually improved on as part of a recent work aimed at assigning levels up to $34\,000\text{ cm}^{-1}$,¹ where an accuracy of 0.03 cm^{-1} was achieved for the same energy limits. However, this fell to 0.04 cm^{-1} for levels up to $25\,000\text{ cm}^{-1}$ when the higher energy levels were include into the fitting procedure. This suggests that attempts to obtain a PES accurate to better than 0.02 cm^{-1} for all available energy levels of water are not possible at the moment. Such a project would require the production of a globally correct *ab initio* PES for water as a precursor to any such fit. Work on such an *ab initio* surface is currently under way.

ACKNOWLEDGMENTS

This work was supported by the Royal Society, EPSRC and the Russian Foundation for Basic Research. S.V.S. ac-

knowledges support from Grant No. MK-1155.2008.2. This research forms part of an effort by a Task Group of the International Union of Pure and Applied Chemistry (IUPAC, Project No. 2004-035-1-100) on "A database of water transitions from experiment and theory."

- ¹P. Maksyutenko, J. S. Muentner, N. F. Zobov, S. V. Shirin, O. L. Polyansky, T. R. Rizzo, and O. V. Boyarkin, *J. Chem. Phys.* **126**, 241101 (2007).
- ²G. Tinetti, A. Vidal-Madjar, M.-C. Liang, J.-P. Beaulieu, Y. Yung, S. Carey, R. J. Barber, J. Tennyson, I. Ribas, N. Allard, G. E. Ballester, D. K. Sing, and F. Selsis, *Nature (London)* **448**, 169 (2007).
- ³O. L. Polyansky, N. F. Zobov, S. Viti, J. Tennyson, P. F. Bernath, and L. Wallace, *Science* **277**, 346 (1997).
- ⁴H. Partridge and D. W. Schwenke, *J. Chem. Phys.* **106**, 4618 (1997).
- ⁵O. L. Polyansky, A. G. Csaszar, S. V. Shirin, N. F. Zobov, P. Barletta, J. Tennyson, D. W. Schwenke, and P. J. Knowles, *Science* **299**, 539 (2003).
- ⁶P. Barletta, S. V. Shirin, N. F. Zobov, O. L. Polyansky, J. Tennyson, E. F. Valeev, and A. G. Csaszar, *J. Chem. Phys.* **125**, 204307 (2006).
- ⁷O. L. Polyansky and J. Tennyson, *J. Chem. Phys.* **110**, 5056 (1999).
- ⁸V. G. Tyuterev, S. A. Tashkun, D. W. Schwenke, P. Jensen, T. Cours, A. Barbe, and M. Jacon, *Chem. Phys. Lett.* **316**, 271 (2000).
- ⁹V. G. Tyuterev, S. A. Tashkun, and D. W. Schwenke, *Chem. Phys. Lett.* **348**, 223 (2001).
- ¹⁰N. F. Zobov, S. V. Shirin, O. L. Polyansky, J. Tennyson, P.-F. Coheur, P. F. Bernath, M. Carleer, and R. Colin, *Chem. Phys. Lett.* **414**, 193 (2005).
- ¹¹P. Dupre, T. Germain, N. F. Zobov, R. N. Tolchenov, and J. Tennyson, *J. Chem. Phys.* **123**, 154307 (2005).
- ¹²P. Maksyutenko, T. R. Rizzo, and O. V. Boyarkin, *J. Chem. Phys.* **125**, 181101 (2006).
- ¹³J. Kauppinen, T. Karkkainen, and E. Kyro, *J. Mol. Spectrosc.* **71**, 15 (1978).
- ¹⁴O. L. Polyansky, N. F. Zobov, S. Viti, and J. Tennyson, *J. Mol. Spectrosc.* **189**, 291 (1998).
- ¹⁵O. L. Polyansky, P. Jensen, and J. Tennyson, *J. Chem. Phys.* **101**, 7651 (1994).
- ¹⁶S. V. Shirin, O. L. Polyansky, N. F. Zobov, P. Barletta, and J. Tennyson, *J. Chem. Phys.* **118**, 2124 (2003).
- ¹⁷S. V. Shirin, N. F. Zobov, O. L. Polyansky, J. Tennyson, T. Parekunnel, and P. F. Bernath, *J. Chem. Phys.* **120**, 206 (2004).
- ¹⁸O. L. Polyansky, P. Jensen, and J. Tennyson, *J. Chem. Phys.* **105**, 6490 (1996).
- ¹⁹S. N. Yurchenko, B. A. Voronin, R. N. Tolchenov, N. Doss, O. V. Naumenko, W. Thiel, and J. Tennyson, *J. Chem. Phys.* **128**, 044312 (2008).
- ²⁰S. V. Shirin, N. F. Zobov, and O. L. Polyansky, *J. Quant. Spectrosc. Radiat. Transf.* **109**, 549 (2008).
- ²¹S. V. Shirin, O. L. Polyansky, N. F. Zobov, R. I. Ovsyannikov, A. G. Csaszar, and J. Tennyson, *J. Mol. Spectrosc.* **236**, 216 (2006).
- ²²L. Wallace, P. Bernath, W. Livingston, K. Hinkle, J. Bustler, B. J. Guo, and K. Q. Zhang, *Science* **268**, 1155 (1995).
- ²³L. Wallace, W. Livingston, K. Hinkle, and P. Bernath, *Astrophys. J. Lett.* **106**, 165 (1996).
- ²⁴O. L. Polyansky, N. F. Zobov, S. Viti, J. Tennyson, P. F. Bernath, and L. Wallace, *Astrophys. J.* **489**, L205 (1997).
- ²⁵O. L. Polyansky, N. F. Zobov, S. Viti, J. Tennyson, P. F. Bernath, and L. Wallace, *J. Mol. Spectrosc.* **186**, 422 (1997).
- ²⁶N. F. Zobov, S. V. Shirin, O. L. Polyansky, R. J. Barber, J. Tennyson, P.-F. Coheur, P. F. Bernath, M. Carleer, and R. Colin, *J. Mol. Spectrosc.* **237**, 115 (2006).
- ²⁷A. D. Bykov, O. V. Naumenko, A. M. Pshenichnikov, L. N. Sinitsa, and A. P. Shcherbakov, *Opt. Spectrosc.* **94**, 528 (2003).
- ²⁸L. Lodi, R. N. Tolchenov, J. Tennyson, A. E. Lynas-Gray, S. V. Shirin, N. F. Zobov, O. L. Polyansky, A. G. Csaszar, J. N. P. Van Stralen, and L. Visscher, *J. Chem. Phys.* **128**, 044304 (2008).
- ²⁹R. B. Wattson and L. S. Rothman, *J. Quant. Spectrosc. Radiat. Transf.* **46**, 763 (1992).
- ³⁰A. E. Lynas-Gray, S. Miller, and J. Tennyson, *J. Mol. Spectrosc.* **169**, 458 (1995).
- ³¹D. Lisak and J. T. Hodges, *J. Mol. Spectrosc.* **249**, 6 (2008).
- ³²See EPAPS Document No. E-JCPSA6-128-046821 for electronic versions of all the potential energy surfaces as FORTRAN programs and for copies of the linelists. For more information on EPAPS, see <http://www.aip.org/pubservs/epaps.html>.

- ³³ J. Tennyson, M. A. Kostin, P. Barletta, G. J. Harris, O. L. Polyansky, J. Ramanlal, and N. F. Zobov, *Comput. Phys. Commun.* **163**, 85 (2004).
- ³⁴ T. Furtenbacher, A. G. Csaszar, and J. Tennyson, *J. Mol. Spectrosc.* **245**, 115 (2007).
- ³⁵ J. Tennyson *et al.*, *J. Quant. Spectrosc. Radiat. Transf.* (unpublished).
- ³⁶ J. Tennyson, N. F. Zobov, R. Williamson, O. L. Polyansky, and P. F. Bernath, *J. Phys. Chem. Ref. Data* **30**, 735 (2001).
- ³⁷ O. Naumenko, M. Snee, M. Tanaka, S. V. Shirin, W. Ubachs, and J. Tennyson, *J. Mol. Spectrosc.* **237**, 63 (2006).
- ³⁸ L. Lodi, O. L. Polyansky, and J. Tennyson, *Mol. Phys.* (to be published).
- ³⁹ D. W. Schwenke, *J. Phys. Chem. A* **105**, 2352 (2001).
- ⁴⁰ N. F. Zobov, R. I. Ovsyannikov, S. V. Shirin, and O. L. Polyanskiy, *Opt. Spectrosc.* **102**, 348 (2007).
- ⁴¹ A. J. C. Varandas and S. P. J. Rodrigues, *Spectrochim. Acta, Part A* **58**, 629 (2002).
- ⁴² J. S. Kain, O. L. Polyansky, and J. Tennyson, *Chem. Phys. Lett.* **317**, 365 (2000).
- ⁴³ M. Vidler and J. Tennyson, *J. Chem. Phys.* **113**, 9766 (2000).
- ⁴⁴ S. Fally, P. F. Coheur, M. Carleer, C. Clerbaux, R. Colin, A. Jenouvrier, M. F. Merienne, C. Hermans, and A. C. Vandaele, *J. Quant. Spectrosc. Radiat. Transf.* **82**, 119 (2003).
- ⁴⁵ R. N. Tolchenov, N. F. Zobov, O. L. Polyansky, J. Tennyson, O. Naumenko, M. Carleer, P.-F. Coheur, S. Fally, A. Jenouvrier, and A. C. Vandaele, *J. Mol. Spectrosc.* **233**, 68 (2005).
- ⁴⁶ L. Lodi and J. Tennyson, *J. Quant. Spectrosc. Radiat. Transf.* **109**, 1219 (2008).
- ⁴⁷ R. J. Barber, J. Tennyson, G. J. Harris, and R. N. Tolchenov, *Mon. Not. R. Astron. Soc.* **368**, 1087 (2006).
- ⁴⁸ O. V. Naumenko, O. Leshchishina, S. Shirin, A. Jenouvrier, S. Fally, A. C. Vandaele, E. Bertseva, and A. Campargue, *J. Mol. Spectrosc.* **238**, 79 (2006).